

SECONDARY FLOW STRUCTURES UNDER STENT-INDUCED PERTURBATIONS FOR CARDIOVASCULAR FLOW IN A CURVED ARTERY MODEL

Autumn L. Glenn, Kartik V. Bulusu, and Michael W. Plesniak
Department of Mechanical and Aerospace Engineering
The George Washington University
801 22nd Street, N.W, Washington, D.C. 20052
plesniak@gwu.edu

Fangjun Shu
Department of Mechanical and Aerospace Engineering
New Mexico State University
MSC 3450, P.O. Box 30001, Las Cruces, NM 88003-8001
shu@nmsu.edu

ABSTRACT

Secondary flows within curved arteries with unsteady forcing are well understood to result from amplified centrifugal instabilities under steady-flow conditions and are expected to be driven by the rapid accelerations and decelerations inherent in such waveforms. They may also affect the function of curved arteries through pro-atherogenic wall shear stresses, platelet residence time and other vascular response mechanisms.

Planar PIV measurements were made under multi-harmonic non-zero-mean and physiological carotid artery waveforms at various locations in a rigid bent-pipe curved artery model. Results revealed symmetric counter-rotating vortex pairs that developed during the acceleration phases of both multi-harmonic and physiological waveforms. An idealized stent model was placed upstream of the bend, which initiated flow perturbations under physiological inflow conditions. Changes in the secondary flow structures were observed during the systolic deceleration phase ($t/T \approx 0.20-0.50$). Proper Orthogonal Decomposition (POD) analysis of the flow morphologies under unsteady conditions indicated similarities in the coherent secondary-flow structures and correlation with phase-averaged velocity fields.

A regime map was created that characterizes the kaleidoscope of vortical secondary flows with multiple vortex pairs and interesting secondary flow morphologies. This regime map in the curved artery model was created by plotting the Dean number against another dimensionless acceleration-based parameter marking numbered regions of vortex pairs.

INTRODUCTION

Arterial fluid dynamics is highly complex; involving pulsatile flow in elastic tapered tubes with many curves and branches. Flow is typically laminar, although more complicated flow regimes can be produced in the vasculature

by the complex geometry and inherent forcing functions, as well as changes due to disease. Strong evidence linking cellular biochemical response to mechanical factors such as shear stress on the endothelial cells lining the arterial wall has received considerable interest (Berger and Jou, 2000; Barakat and Lieu, 2003; White and Frangos, 2007; Melchior and Frangos, 2010). Secondary flow structures may affect the wall shear stress in arteries, which is known to be closely related to atherogenesis (Mallubhotla et al., 2001; Evegren et al., 2010).

In curved tubes, secondary flow structures characterized by counter-rotating vortex pairs (Dean vortices) are well-understood to result from amplified centrifugal instabilities under steady flow conditions. Standard Dean vortices are manifested as a pair of counter-rotating eddies with fluid moving outwards from the center of the tube, away from the radius of curvature of the bend and circulating back along the walls of the tube (Dean, 1927; Dean, 1928).

Under unsteady, zero-mean, harmonic, oscillating conditions, flow in the same bend results in the confinement of viscosity to a thin region near the walls (Stokes' layer) and exhibits entirely different secondary flow patterns. When the radius of the tube is large compared with the Stokes' layer thickness, vortical structures in the Stokes' layer rotate in the same directional sense as the Dean vortices in the steady flow case. This rotation drives the fluid in the inviscid core to generate the inward-centrifuging Lyne vortices (Lyne 1970). For flow forced in a zero-mean sinusoidal mode, Lyne's perturbation analysis (with Stokes' layer thickness as the perturbation parameter) predicted that inward centrifuging occurs at Womersley numbers greater than 12. In curved tubes with sufficiently high unsteady forcing frequency, secondary flow development is dominated by the near-wall viscous Stokes' layer (Lyne, 1970). In addition, bifurcation of Dean vortices into three or more vortices has been observed in

bent tubes and channels with pulsatile flow (Mallubhotla *et al.* 2001, Belfort *et al.* 2001).

In a fundamental sense, secondary flows are important because they may significantly alter boundary layer structure (Ligrani and Niver, 1988) and in arteries may affect the wall shear stress and platelet residence time which is important in arterial disease (Mallubhotla *et al.*, 2001; Weyrich *et al.*, 2002).

The creation of a regime map to characterize Dean vortices has been attempted for steady inflow conditions and Dean numbers up to 220 and later extended to 430 by Ligrani and Niver (1988) and Ligrani (1994). A transition of a two-vortex Dean-type system into a bifurcating four-vortex Dean-type system is described by Mallubhotla *et al.* (2001) in another domain map. For pulsatile flow conditions the creation of a flow regime map has been attempted in related bioengineering applications, *e.g.*, classification of flow patterns in a centrifugal blood pump (Shu *et al.*, 2008; Shu *et al.*, 2009). Their research emphasized the importance of pulsatility in curved tubes and the associated time derivative of the flow rate (dQ/dt) on hemodynamics within clinical scale Turbodynamic Blood Pumps (TBPs). A regime map was developed for the ensuing pulsatile flow conditions that provided a preclinical validation of TBPs intended for use as ventricular assist devices.

The observed correlation between vascular response and mechanical stimuli has been the impetus for many fluid mechanics investigations of geometries known to be pathological or pro-atherogenic, such as stenoses (Ahmed and Giddons, 1983; Berger and Jou, 2000; Peterson, 2006). Consequently, it is necessary to investigate secondary flows in a bend subjected to unsteady non-zero-mean flow forcing that will be relevant cardiovascular flows. The importance of the ongoing research and study presented in this paper is the creation of a regime map that characterizes secondary flows based on the forcing flow waveform alone. Flow waveforms are easier to measure compared to velocity fields. Clinical implications of such studies include characterization of secondary flow morphologies based on patient-specific flow waveforms.

The main objective of the study presented in this paper is to characterize the secondary flow morphologies based on the Dean number and another non-dimensional parameter which characterizes the driving waveform. The Dean number relates centrifugal forces to viscous forces and is given by equation (1).

$$D = \frac{Ud}{\nu} \sqrt{\frac{d}{2R}} \quad (1)$$

where U is the velocity in the primary flow direction, d is the pipe inner diameter, ν is the kinematic viscosity of the fluid, and R is the radius of curvature. The physiological flow

waveform used in this study is based on ultrasound and ECG measurements of blood flow made by Holdsworth *et al.* (1999) within the left and right carotid arteries of 17 healthy human volunteers. Peterson and Plesniak (2008) found that the secondary flow patterns in the circular bend strongly depend on the forcing flow waveform. Thus, the geometry, flow forcing, and secondary flows studied were representative of flow in arterial blood vessels. In addition, three multi-harmonic waveforms were also used to better understand the nature and persistence of secondary flows.

EXPERIMENTAL FACILITY

A schematic diagram of the experimental facility is shown in Figure 1. A test section was specially designed to enable Particle Image Velocimetry (PIV) measurements of secondary flow at five locations within the bend. The test section consisted of an 180° bend formed from two machined acrylic pieces. Pipes of 12.7 mm inner diameter were attached to both the inlet and outlet of the test section with lengths of 1.2 meters and 1 meter, respectively, to ensure that fully developed-flow entered the test section. A stent model could be installed between the test section and the inlet pipe. Experiments were conducted with an idealized stent model to observe the effects of perturbations on the secondary flow characteristics. The idealized stent model consisted of an array of equi-spaced o-rings that protruded into the flow (by half of the o-ring diameter, 3.175 mm). A programmable gear pump (Ismatec model BVP-Z) was used to drive the flow.

The voltage waveform generated to control the pump speed was supplied by a data acquisition card (National Instruments DAQ Card-6024E) using a custom virtual instrument written in LabView. A trigger signal for the PIV system was generated by the same data acquisition module to synchronize measurements. A refractive index matching fluid was used in the experiments to minimize optical distortion of

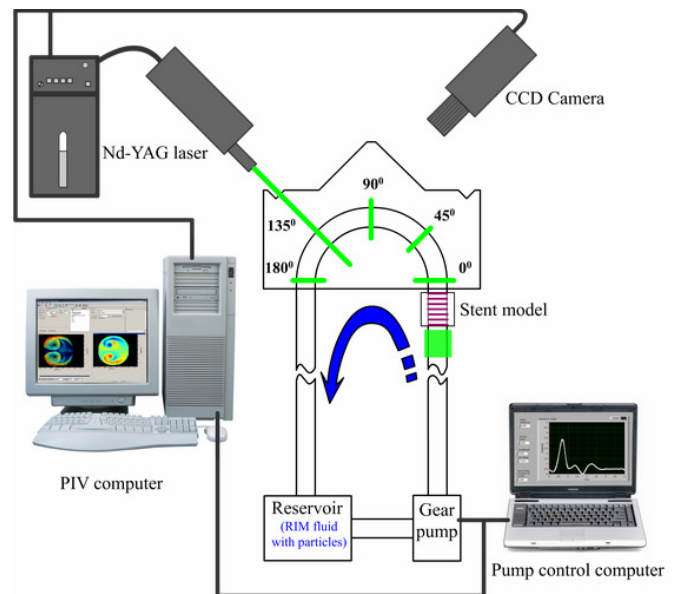


Figure 1: Experimental Setup

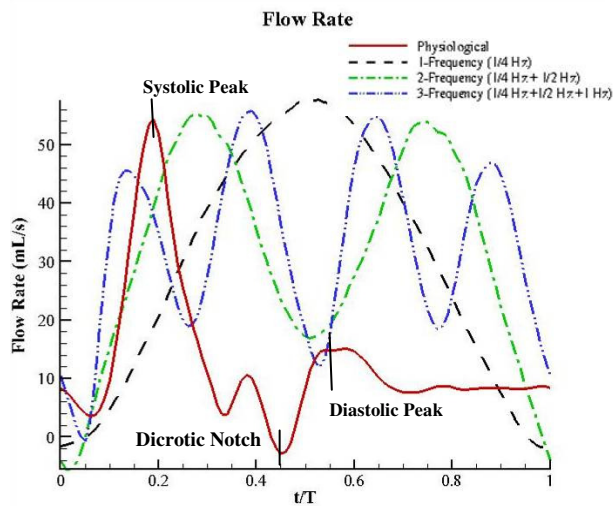


Figure 2: Experimental Flow Forcing Waveforms

Table 1: Tabulated Reynolds and Dean Values for Experimental Waveforms

	Physiological	1-Frequency	2-Frequency	3-Frequency
Re_{max}	1655	1658	1516	1508
Re_{ag}	383	839	841	871
D_{max}	626	626	573	570
D_{avg}	145	317	318	329

the particle image. The fluid was composed of 79% saturated aqueous sodium iodide, 20% pure glycerol, and 1% water by volume with a refractive index of 1.49 at 25°C. The fluid kinematic viscosity was 3.55 cSt ($3.55 \times 10^{-6} \text{ m}^2/\text{s}$), which closely matches that of blood. To eliminate glare from boundary, spherical fluorescent particles with mean diameter

of $7\mu\text{m}$ were used to seed the fluid for PIV measurements.

Four waveforms were used to force the flow (Figure 2): physiological, 1-frequency sinusoidal, 2-frequency multi-harmonic, and 3-frequency multi-harmonic. The physiological waveform is characterized by increased volumetric flow during the systolic phase when the blood is ejected from the heart. The dicrotic notch, which reflects the cessation of systole, occurs at the minimum volumetric flow and is followed by the diastolic phase.

The three other waveforms studied were a $1/4$ Hz sine wave (1-frequency), a $1/4$ Hz sine wave and $1/2$ Hz sine wave superimposed (2-frequency), and a $1/4$ Hz, $1/2$ Hz, and 1 Hz superimposed (3-frequency). All three of these waveforms maintained the physiological period (Womersley number) and amplitude. Reynolds number and Dean number were calculated based on the bulk velocity measured upstream of the bend, and are shown in Table 1. Results and analysis of secondary flow structures at 90° location are presented.

Flow rate was calculated by integrating the velocity profiles (which was measured using the 2-D PIV system) across the diameter of the pipe, upstream of the bend. The period of the waveform was 4 seconds, which is scaled based on physiological Womersley number (α) of 4.2.

RESULTS

Data were first acquired without a stent model in the flow. The evolution of vortices under the physiological inflow waveform is shown in Figure 3. The large-scale coherent secondary-flow structures were similar under all four waveforms. During the acceleration phase in each waveform, two symmetric counter-rotating vortices located near the inner wall of the bend were observed (Figure 3). With increasing flow rate, the primary (large-scale) vortices, tend to move toward the inner wall against the centrifugal force. As inflow conditions neared a peak flow rate, these structures evolved into two pairs of counter rotating symmetric vortices (four vortices). Unlike Lyne-type vortices, the first vortex pair was

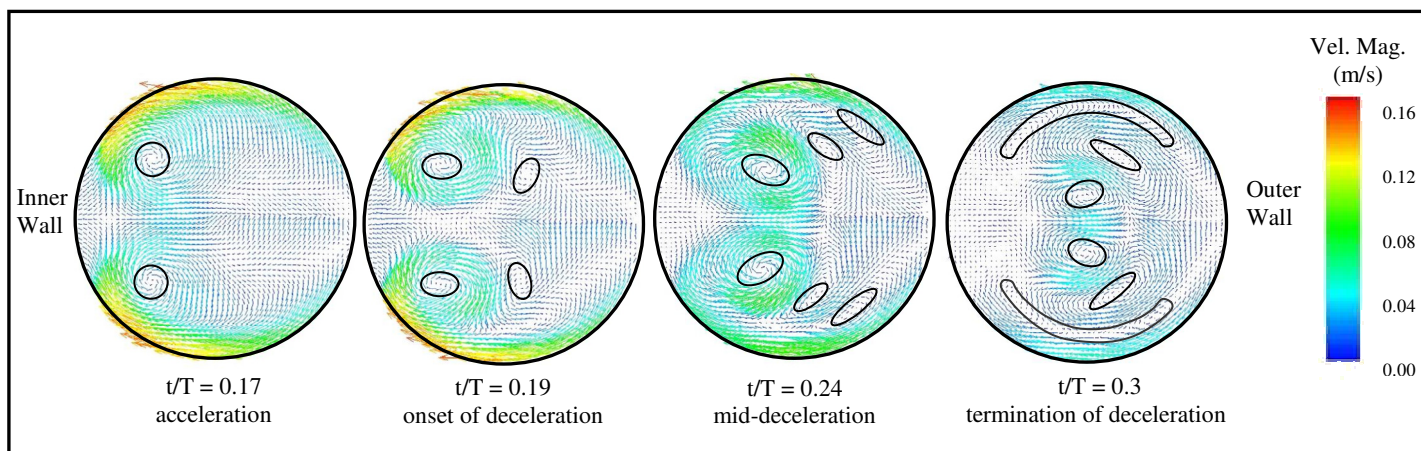


Figure 3: Vector Plot Showing the Evolution of Secondary Flow Vortices under Physiological Forcing

not confined to the boundary layer but instead was only partially deformed while remaining near the inner wall of the bend. As the flow began to decelerate, the vortices break into six symmetric vortices, three pairs. These six vortices persist throughout deceleration, though their arrangement changes. During deceleration, six vortices were arranged in a symmetric 'V' shape and the smaller vortices near the top and bottom of the outer wall. As deceleration continued, the partially deformed primary vortices tend to move towards the outer wall of the pipe along the direction of the centrifugal force. As the two primary vortices moved towards the center, the smaller vortices undergo deformation with one pair elongating along the top and bottom of the pipe as in the Lyne-type vortices. It can therefore be concluded that the large-scale (primary) vortices undergo translation and smaller vortices undergo deformation due to centrifugal forces (Figure 3).

Under physiological forcing, the six vortices persisted until the beginning of diastolic acceleration. The diastolic flow rates are smaller than the systole and the coherent structures quickly broke down as the flow rate reached its minimum. With the onset of systolic acceleration, the two vortex patterns were initiated again and the cycle repeated itself.

It was observed that the vortex formation exhibited a similar pattern across all waveforms tested. This led to the hypothesis that these flows can be characterized to allow prediction of the morphology of the secondary flow based on flow waveform which can be measured for individual patients.

In general, secondary flow structures develop because of an imbalance of centrifugal and viscous forces. As a result, Dean number was one parameter considered in creating a regime map to characterize the vortex pairs in the various waveforms. Unlike for steady flow, Dean number alone was not a sufficient parameter to quantify the coherent structures and develop a regime map. Another parameter indicative of rapid accelerations and decelerations inherent in pulsatile inflow conditions is necessary. The following dimensionless acceleration parameter (DAP) was developed.

$$DAP = \left(\frac{dU}{dt} \right) \frac{(d)(T)}{v} \sqrt{\frac{d}{2R}} \quad (2)$$

where T is the period, and the acceleration is represented by the time-rate-of-change of the velocity $\left(\frac{dU}{dt} \right)$ in the primary flow direction. Centerline velocity was used to calculate both the Dean number (D) and (DAP). This parameter allows for comparison of acceleration among different waveforms. These two parameters were used to

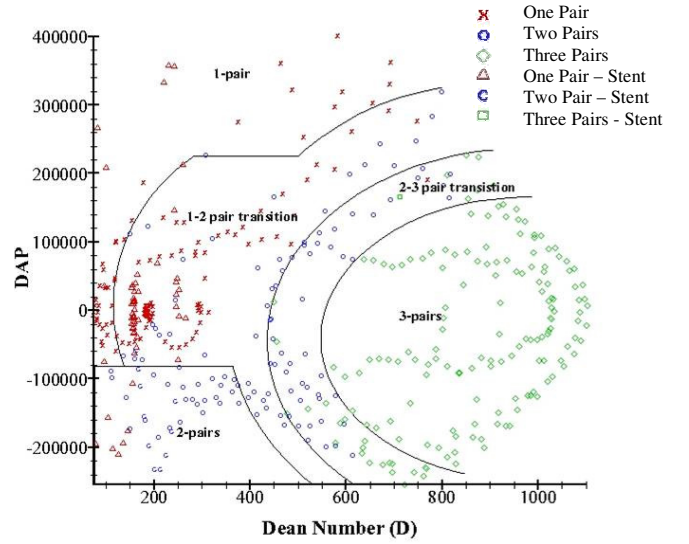


Figure 4: Regime map showing areas of 1, 2, and 3 symmetric vortex pairs and transition regions from 1-to-2 and 2-to-3 vortex pairs.

create a regime map (Figure 4) of the secondary flow morphologies.

In order to populate this regime map secondary flows were characterized by the number of symmetric vortex pairs identified visually. The values were then mapped on a plot of Dean number (morphologies) vs. DAP (Figure 4). In this regime map the distinct vortex pairs are visible during deceleration (negative vertical axis) and there are also well defined regions of transition from 2 pairs to 3 pairs. During acceleration (positive vertical axis) however, the vortex pairs are still developing and, therefore, transition region is predominant.

Experiments with a model of an idealized stent inserted upstream to the bend were also performed with the physiological inflow waveform. Large-scale structures in the systolic acceleration phase of the physiological flow with the idealized stent were observed to be very similar to those in flow without the stent model (Figure 5). The idealized stent model initiated spatial and temporal perturbations that enhanced the breakdown of large-scale secondary flow structures, mainly in the deceleration phase in the flow. In the instantaneous velocity flow fields during deceleration, multiple asymmetric vortical structures were present. However, phase-averaged vortical structures appeared to possess symmetric geometries similar to the results without a stent (Figure 5).

Further analysis using Proper Orthogonal Decomposition (POD) of velocity fields confirmed the presence of large-scale coherent structures, demonstrating correlation with the structures, appearing in the systolic deceleration phase (Figure 6). The POD results revealed that the first five eigenmodes contained approximately 91% of the energy in the

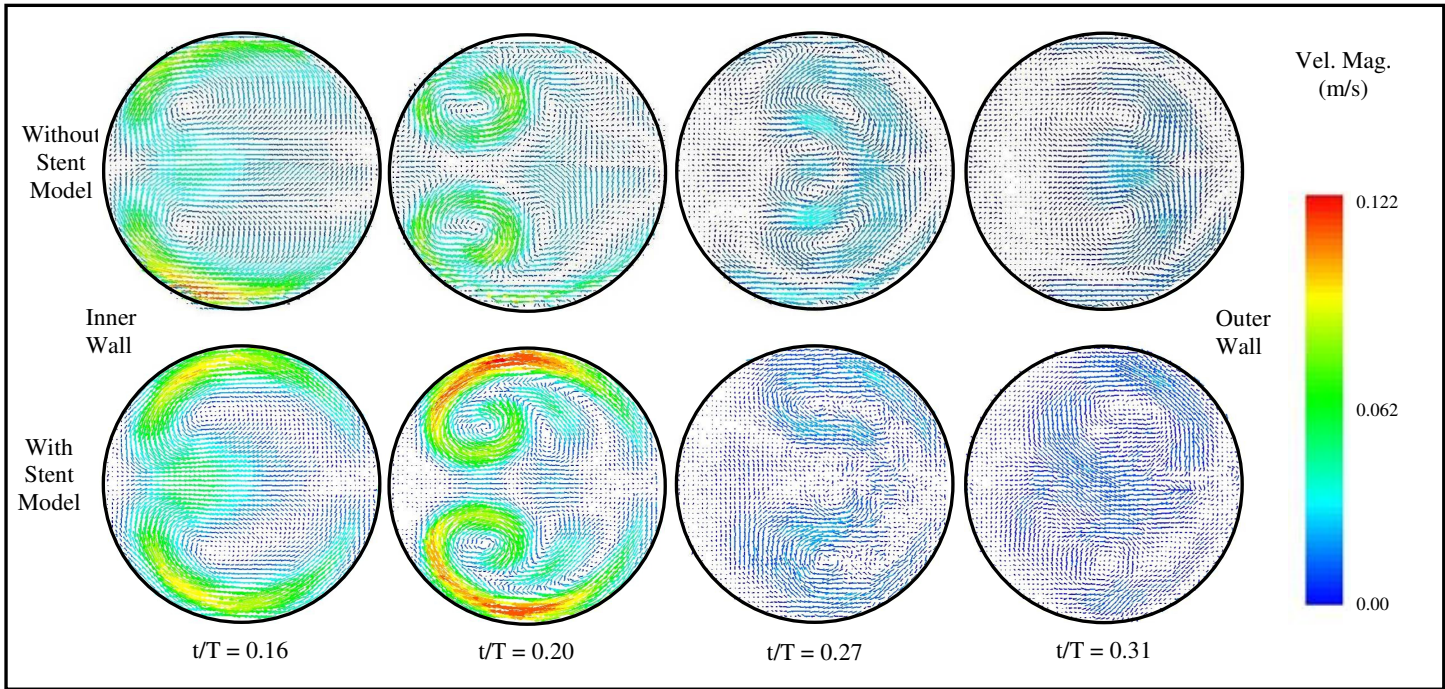


Figure 5: Comparison of secondary flow under physiological forcing, with and without stent model

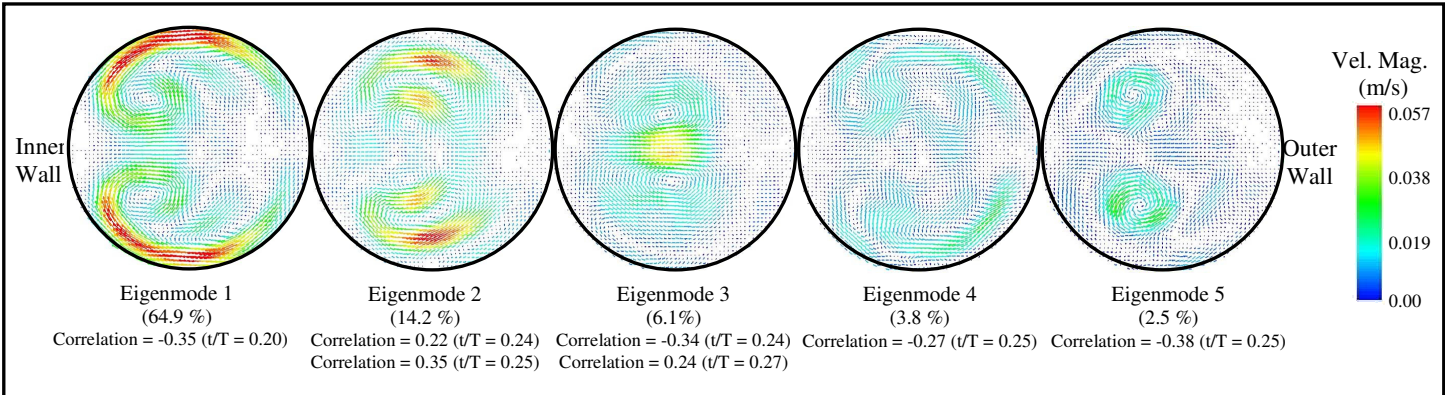


Figure 6: First five eigenmodes resulting from POD method

secondary flow and correlated well with phase averaged velocity fields during systolic deceleration. Accordingly, it can be inferred that despite stent-induced perturbations, the large-scale structures still persist and may have the potential to initiate vascular response mechanisms.

Although the flow characteristics appeared to be similar, when plotted on the regime map, the stent data did not fit into the previously defined regions. The stent changed the effective diameter of the pipe and, therefore, the Dean number (D) and DAP . When Dean number (D) and DAP were calculated, using an effective diameter of 10.7 mm, the inner diameter of the stent struts, and then plotted on the regime map, the data fit into the previously-defined regions well.

The regime map was created based on number of vortex pairs identified visually, which is very subjective at some phases. With help of POD, the secondary flow could be expressed by combinations of eigenmodes. POD analysis and other higher order methods will provide a more objective and accurate process in creating the regime maps for unsteady forcing in the future.

CONCLUSIONS

The morphology of the secondary flow becomes more complex with increased Dean number and acceleration plays an important role in the formation of the secondary flow structures. A regime map was developed using the Dean

number and a dimensionless acceleration-based parameter (*DAP*). Under flow forcing conditions without the stent model distinct regions of vortex pairs (one, two and three pairs symmetric vortices) were identified on the regime map, thereby allowing the characterization of secondary flow structures. In addition, regions representing transition from 1-to-2 and 2-to-3 secondary flow vortex pairs were also represented in the regime map.

The idealized stent model was found to cause disturbances in the flow that led to changes in the morphology of secondary flow structures. POD analysis of phase-averaged velocity fields under physiological forcing during systolic deceleration showed that the large-scale secondary flow structures did not change significantly, even with minor disturbances present in the flow due to an idealized stent model. The protrusions from the stent model located upstream of the bend, changed pipe diameter. The effective diameter inside of the stent must be used to characterize secondary flow structures in the regime map.

For steady flows, Dean number is adequate to describe secondary flow morphologies. In contrast, for flows with unsteady forcing and its inherent rapid accelerations and decelerations a single parameter such as Dean number alone, cannot adequately describe the secondary flow morphologies. The dimensionless acceleration-based parameter (*DAP*) was required in addition to the Dean number to describe secondary flow morphologies. It characterizes the flow acceleration.

REFERENCES

- Ahmed, S. A., and Giddens, D. P., 1983, "Velocity measurements in steady flow through axisymmetric stenoses at moderate Reynolds numbers," *Journal of Biomechanics*, Vol. 16 pp. 505-516.
- Belfort, G., Mallubhotla, H., Edelstein, W.A., and Early, T.A., 2001, "Bifurcation and Application of Dean Vortex Flow," *12th International Couette-Taylor Workshop*, Evanston, IL USA.
- Evegren, P., Fuchs, L., and Revstedt, J., 2010, "On the Secondary Flow Through Bifurcating Pipes," *Phys. Fluids*, Vol. 22, Issue 10.
- Berger, S. A., and Jou, L-D., 2000, "Flows in stenotic vessels," *Annual Review of Fluid Mechanics*, Vol 32 pp. 347-382.
- Dean, W.R, Hurst, J.M., 1927, "Note on the Motion of Fluid in a Curved Pipe," *Mathematika*, Vol. 6 pp 77-85.
- Dean, W.R., 1928, "The Stream-line Motion of Fluid in a Curved Pipe," *The London, Edinburgh, and Dublin Philosophical Magazine and Journal of Science*, Vol. 7 pp 673-695.
- White, C.R. and Frangos, J. A., 2007, "The shear stress of it all: the cell membrane and mechanochemical transduction," *Phil. Trans. R. Soc. B*, 362, pp. 1459-1467.
- Holdsworth, D.W., Norley, C. J. D, Frayne, R., Steinman, A., and Rutt, B.K., 1999, "Characterization of common carotid artery blood-flow waveforms in normal human subjects," *Physiological Measurements*, Vol. 20 pp. 219-240.
- Melchior, B., Frangos, J.A., 2010, "Shear-induced endothelial cell-cell junction inclination," *Am. J. Physiol. Cell Physiol.*, Vol. 299, C621-C629.
- Ligrani, P.M. and Niver, R.D., 1988, "Flow Visualization of Dean Vortices with 40 to 1 aspect ratio," *Phys. Fluids*, Vol. 31(12) pp. 3605-3617.
- Ligrani, P. M., 1994, "Study of Dean Vortex Development and Structure in a Curved Rectangular Channel With Aspect Ratio of 40 at Dean numbers up to 430," *NASA Contractor Report 4607, ARL Contractor Report ARL-CR-144*.
- Lyne, W. H., 1970, "Unsteady viscous flow in a curved pipe," *Journal of Fluid Mechanics*, Vol. 45 pp. 13-31.
- Mallubhotla, H., Belfort, G., Edelstein, W.A., and Early, T.A., 2001, "Dean Vortex Stability Using Magnetic Resonance Flow Imaging and Numerical Analysis," *AICHE Journal*, Vol. 47(5) pp. 1126-1139
- Peterson, S. D., 2006, *On the effect of perturbations on idealized flow in model stenotic arteries*, Ph.D. Dissertation, Purdue University
- Peterson, S.D. and Plesniak, M. W., 2008, "The influence of inlet velocity profile and secondary flow on pulsatile flow in a model artery with stenosis," *Journal of Fluid Mechanics*, Vol. 616 pp. 263-301.
- Shu, F., Vandenberghe, S., Miller, P.J. and Antaki, J.F., 2008, "Comprehensive classification of flow patterns in a centrifugal blood pump under pulsatile conditions," *16th Congress of the International Society for Rotary Blood Pumps (ISRBP), Artif. Organs 2009*, Vol. 33(6):A89 October 2-4, Houston, TX, USA.
- Shu, F., Vandenberghe, S., and Antaki, J.F., 2009, "The Importance of dQ/dt on the Flow Field in a Turbodynamic Pump With Pulsatile Flow," *Artificial Organs*, Vol. 33(9) pp. 757-762.
- Barakat, A.I. and Lieu, D. K., 2003, "Differential Responsiveness of Vascular Endothelial Cells to Different Types of Fluid Mechanical Shear Stress," *Cell Biochemistry and Biophysics*, Vol. 38, pp. 323-344.
- Weyrich, A.S., Prescott, S.M., and Zimmerman, G.A., 2002, "Platelets, endothelial cells, inflammatory chemokines, and restenosis: complex signaling in the vascular play book," *Circulation*, Vol. 106 (12) pp 1433-1435